The Egyptian Journal of Hospital Medicine (July 2025) Vol. 100, Page 2769-2778

The Role of Ovarian–Reporting and Data System MRI Classification (MRI O-RADS) in the Evaluation of Ovarian Lesions

Belal Said Soltan, Mohamed Shawky Abdullah, Rabab Ibrahim Yasin,
Esraa Mohamed Saied Abdelwahed Rashed*, Safaa Aboelkasem Mohamed Soliman
Diagnostic and Interventional Radiology and Medical Imaging Department,
Faculty of Medicine, Menoufia University, Menoufia, Egypt
***Corresponding author:** Esraa Mohamed Saied, **Mobile:** (+20)1029328963, **Email:** esraarashed13@gmail.com

ABSTRACT

Background: Adnexal masses are a common occurrence in gynecological practice and differentiating between benign and malignant lesions is crucial for effective treatment. Magnetic resonance imaging (MRI) offers superior soft-tissue characterization compared to ultrasound. The Ovarian-Adnexal Reporting and Data System for MRI (O-RADS MRI) is a standardized approach launched to enhance risk categorization of adnexal masses. Its utility in daily clinical practice to predict malignancy is being increasingly recognized.

Objectives: This study aimed to evaluate the diagnostic accuracy of O-RADS MRI classification in assessing ovarian lesions and correlate MRI findings with final histopathological results or after follow-up.

Patients and methods: This prospective study included 50 female patients with ovarian lesions who were referred to the Department of Diagnostic and Interventional Radiology and Medical Imaging at Menoufia University Hospitals by the Department of Gynecology. The study was conducted over a one-year period starting in November 2023.

Results: The mean age of patients was 44.04 ±17.51 years. Pelvic pain was the most common presenting symptom (70%), and the most common lesion was large solid portions without dark-dark features (40%). O-RADS MRI scores were distributed as follows: score 2 (14%), score 3 (18%), score 4 (38%), and score 5 (30%). Final pathological outcomes revealed 68% malignant and 32% benign lesions. ROC analysis yielded a sensitivity of 94%, specificity of 87%, accuracy of 92%, PPV of 88%, and NPV of 94% in predicting malignancy, area under the curve (ROC) is 0.949.

Conclusions: It could be concluded that O-RADS MRI scoring system is a reliable tool with high diagnostic accuracy in differentiating malignant from benign ovarian masses. Its implementation can enhance decision-making and improve patient management.

Keywords: O-RADS, MRI, Ovarian lesions, Ovarian cancer.

INTRODUCTION

In routine clinical practice, ovarian masses are frequently observed and may be discovered by chance in individuals who exhibit symptoms. An ovarian lesion's characterization is a diagnostic problem that is crucial to the preoperative planning of appropriate treatment operations and may have an impact on the patient's care [(1)]. A multidisciplinary approach based on physical examination, laboratory testing, and imaging methods is necessary for the best evaluation of an adnexal mass [(1)].

The first and most crucial imaging technique for ovarian cancer diagnosis is still ultrasound (US). US needs a skilled examiner who can evaluate both the abdomen and the pelvis, despite mounting evidence that it is an accurate method for staging and monitoring ovarian cancer [(2)]. The most used imaging technique for preoperative staging and follow-up is computed tomography (CT) [(2)].

Particularly in individuals with ambiguous lesions, MRI is a crucial problem-solving technique for identifying the origin of a pelvic mass and subsequently characterizing an adnexal mass. Local invasion can also be reliably detected by MRI. High contrast resolution with great soft tissue contrast and the absence of ionizing radiation exposure are the primary benefits of MRI, which is especially significant for young female patients [(3)].

Positron emission tomography integrated with CT is the superior imaging modality for suspected recurrence, especially in women with elevated cancer antigen 125 (CA125) levels, despite negative findings from traditional imaging techniques [(2)].

The ovarian-adnexal reporting and data system on magnetic resonance imaging (O-RADS MRI) risk classification approach was created by the O-RADS MRI Committee, a worldwide collaborative effort led by the American College of Radiology and including a varied collection of adnexal imaging and treatment specialists [(4)]. An accepted method for classifying pelvic gynecological tumors according to their risk of cancer is the O-RADS MRI score [(5)].

The challenge in treating adnexal masses is to prevent both overdiagnosis of benign lesions, which can result in needless surgery and jeopardize fertility, and underdiagnosis of malignant lesions, which suggests a poor prognosis and immediate treatment [(6)].

The risk of infertility following surgery for benign ovarian cysts has been well established [(5)], and the incidence of malignancy in women having ovarian surgery is rather low, particularly if the procedure is performed solely on the basis of US results [(7)].

Because of the possibility of upstaging a limited early-stage ovarian cancer or the possibility of sample mistake leading to a missed cancer diagnosis,

Received: 14/02/2025
Accepted: 15/04/2025

percutaneous biopsy of a suspected adnexal tumor is not recommended [8].

This study aimed to evaluate the diagnostic accuracy of O-RADS MRI classification in assessing ovarian lesions and correlate MRI findings with final histopathological results or after follow-up.

PATIENTS AND METHODS

This prospective study included 50 female patients with ovarian lesions who were referred to the Diagnostic and Interventional Radiology and Medical Imaging Department at Menoufia University Hospitals by the Department of Gynecology. The study was conducted over a one-year period starting in November 2023.

Inclusion criteria: Patients with ovarian lesions detected on US or CT showing any of the following features: complex ovarian lesions, cystic lesions with solid vegetations, thick septations or soft tissue components, solid ovarian lesions, simple cystic ovarian lesions, or lesions containing pure fatty components.

Exclusion criteria: Patients who suffered from claustrophobia, had poor renal function, or had any general contraindications to MRI (such as the presence of metallic clips or pacemakers).

All patients had a complete clinical examination, which included

- Full history taking with special emphasis on age and menstrual history, as well as any past history of gynecological problems or surgeries.
- Each patient underwent pelvic ultrasonography either trans-abdominal and/or transvaginal (TV) followed by MRI evaluation.
- Final diagnosis was established through histopathological evaluation or follow-up.

METHODS

All patients had preliminary pelvic US utilizing both transabdominal and transvaginal techniques with GE Logic E10 (3-4 MHz and 7-8 MHz probes). Trans-abdominal scans were performed with a full bladder to improve visualization, while trans-vaginal scans were done with an empty bladder for better proximity to the ovaries. Color Doppler was used when needed to assess solid components.MR imaging:

MRI was done with a 1.5 Tesla TOSHIBA MRI scanner. All patients were imaged in the supine position utilizing the pelvic phased array coil.

Proper patient preparation was essential for optimal MRI quality, including psychological reassurance about the scanner environment, assessment of renal function, and removal of all metallic or paramagnetic items.

MRI Protocol:

Pelvic MRI was performed using pre- and post-contrast sequences. The field of view (FOV) included the full mass and adjacent pelvic tissues, not only the solid component.

Sequences:

- **Pre-contrast:**
  - Sagittal, axial, and coronal T2-weighted fast spin-echo
  - Axial T1-weighted fast spin echo with and without fat suppression.
- **Post-contrast:**
  - Axial T1-weighted fast spin echo with fat suppression.
- **Diffusion weighted image (DWI):** DWI was done in the axial plane before contrast administration using single-shot echo-planar sequence with b-values of 0, 800, and 1000.
- **Dynamic contrast-enhanced imaging**: was performed using T1 fat-saturated sequences immediately after manual injection of gadolinium (0.1 mmol/kg, max 20 mL). Images were acquired every 30-40 seconds, covering the selected FOV.
- **Non dynamic contrast-Enhanced MRI:** Axial and coronal T1-weighted images were obtained in the delayed post-contrast phase.

MR Image Analysis

MR sequences were analyzed for lesion:

- Laterality, morphology (cystic, solid, or mixed).
- Signal intensity,
- Wall characteristics.
- Septations.
- Solid components.
- Enhancement.

Assessment also included pelvic invasion, ascites, and peritoneal or omental deposits.

Benign lesions appeared as simple cysts (low T1/high T2 signal, no solid component). Complex benign lesions showed high T1 signal due to fat or blood, distinguishable on fat-suppressed sequences.

Malignant features included wall/septal thickness >3 mm, solid vegetations >1 cm, necrosis, and signs of tumor spread.

DWI analysis differentiated benign from malignant lesions based on signal behavior: benign lesions showed low DWI signal and high apparent diffusion coefficient (ADC) signal (facilitated diffusion), while malignant lesions showed high DWI signal and low ADC signal (restricted diffusion).

Post-contrast images were used to evaluate enhancement of solid tissue, tumor walls, septations, and vegetations.

Dynamic contrast enhanced (DCE)-MRI was analyzed qualitatively using region of interest (ROI) technique. ROIs were placed in the solid tumor and myometrium as reference.

Time-intensity curves were classified as:

- **Type 1:** Gradual enhancement (benign).
- **Type 2:** Moderate rise with plateau (possibly malignant).
- **Type 3**: Rapid rise (likely malignant).

Lesions with type 2 or 3 curves were suggestive of malignant behavior, while type 1 indicated benign vascularity.

Ethical approval:

This study was ethically approved by Menoufia University's Research Ethics Committee. Written informed consent of all the participants was obtained. The study protocol conformed to the Helsinki Declaration, the ethical norm of the World Medical Association for human testing.

Statistical analysis

SPSS version 26 was utilized for the analysis and tabulation of the data. Quantitative data were reported as median and interquartile range for non-normal distributions, or mean ± SD for regularly distributed variables, while descriptive statistics described qualitative data as numbers and percentages.

To compare categorical variables for inferential analysis, the X^2-test and Fisher's- test were utilized; Fisher's exact was employed when anticipated cell counts were low.

For non-parametric comparisons, the Mann-Whitney U test was employed, whereas the Student's t-test was used to compare the means of quantitative data that was regularly distributed. Diagnostic performance was assessed through Receiver Operating Characteristic (ROC) curve analysis, calculating the area under the curve (AUC), sensitivity, specificity, diagnostic accuracy, positive predictive value (PPV), and negative predictive value (NPV).

Cohen's kappa coefficient measured inter-rater agreement, interpreted as poor (<0.20) to perfect (0.81–1.00) agreement. Statistical significance was set at $p < 0.05$.

RESULTS

This study included 50 patients with mean of age of 44.04 ±17.51 years, 60% are post menopause and 40% are pre menopause.

Pelvic pain was the most prevalent complaint affecting 70% of participants, while abdominal swelling occurred in 32%, infertility in 6%, vaginal bleeding in 12% and urinary symptoms in 16%. there were no statistically significant differences between benign and malignant groups regarding symptoms (Table 1).

Table (1): Clinical characteristics of the studied participants (n=50)

Variable	**No. of the studied participants=50**	
	No.	**%**
Pelvic pain		
Present	35	70.0
Absent	15	30.0
Abdominal swelling		
Present	16	32.0
Absent	34	68.0
Infertility		
Present	3	6.0
Absent	47	94.0
Vaginal bleeding		
Present	6	12.0
Absent	44	88.0
Urinary tract symptoms		
Present	8	16.0
Absent	42	84.0
Menstruation		
Pre-menopausal	30	60.0
Post-menopausal	20	40.0

Most of adnexal lesions were unilateral (68%) with an average 1.31+/-0.47 per patient, the most common lesion subtype was large solid component without "dark- dark "features about 40% **(figure 1),** followed by lesions with irregular septation or wall (28%) other types (cystic, septated, papillary, nodules) remaining 32%. Peritoneal implants appeared in 14% of all cases 20.6 % of malignant cases**.**

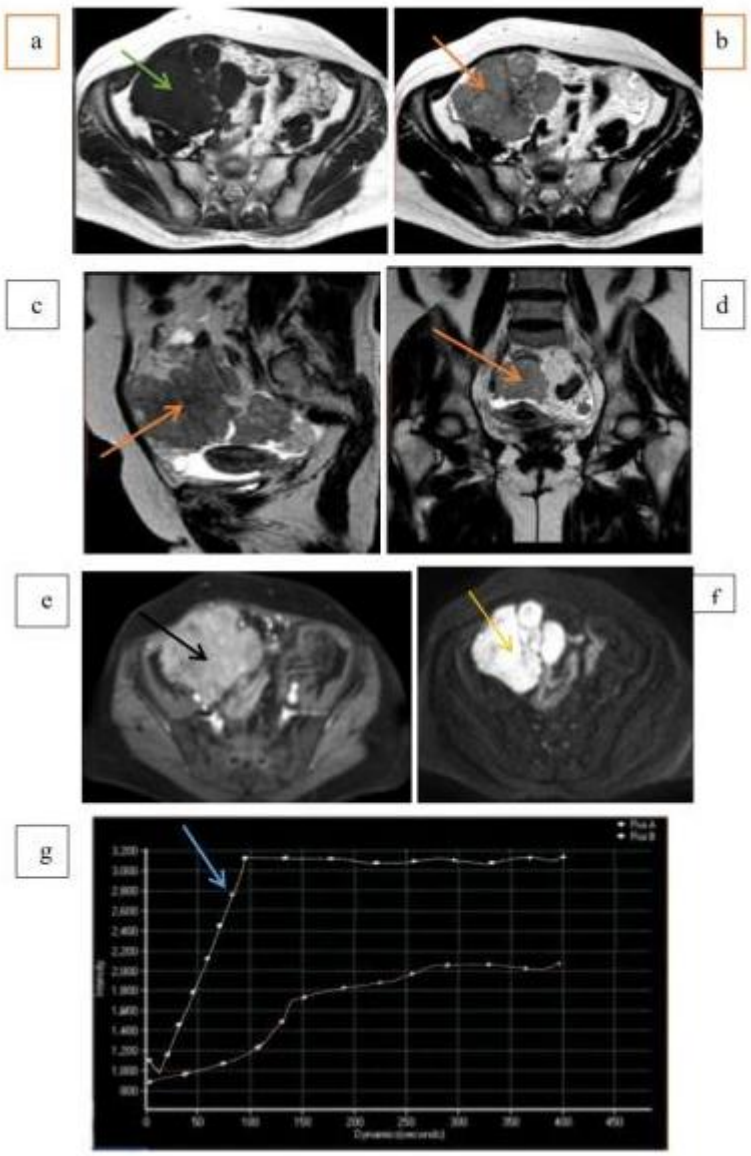

Figure (1): Female patient 53 years old presented with pelvic pain and pelvi-abdominal swelling. US revealed right heterogeneous mass with cystic breakdown. Ascites was noted. MRI was done. Conventional MRI show a large rather defined heterogeneous solid lesion with cystic components. It attains (a) axial T1WI hypointense signal (green arrow). (b, c, d) axial, sagittal, coronal T2WI isointense signal(orange arrow). (e) Post contrast axial T1 fat sat demonstrates moderate enhancement of the lesion (black arrow). (f) axial DWI demonstrates strong diffusion restriction of the lesion(yellow arrow). DCE MRI based diagnosis shows early and more intense increasing enhancement than the myometrium (Type 3 curve (g)) (blue arrow). also it shows omental deposits Management (Surgical): Laparotomy with radical hysterectomy and BSO, O-RADS MRI score: **5** , Pathological diagnosis: Ovarian clear cell carcinoma.

Time intensity curve (TIC) mean=2.31+/- 0.58, malignant cases are with type 4 and 5, most cases are TIC type 4 about **(figure 2).**

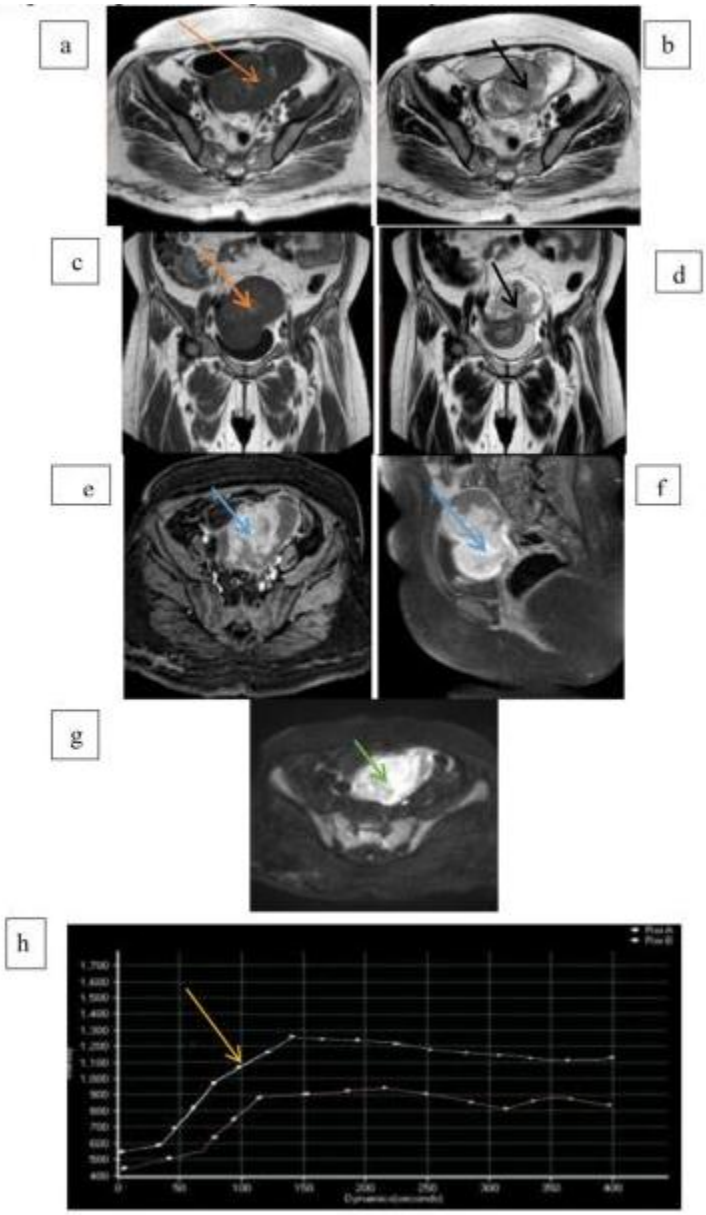

Figure (2): Female patient 52 years old complaining of pelvic pain and swelling. US revealed large left cystic adnexal lesion with solid components. MRI was done, Conventional MRI revealed a large left adnexal cystic mass with irregular soft tissue component. It attains (a) axial and (c) coronal T1WI heterogeneous low signal (orange arrow). And (b) axial and (d) coronal T2WI heterogeneous high signal intensity (black arrow). (e,f) post-contrast axial, sagittal T1WI fat sat shows intense heterogeneous enhancement of the solid component (blue arrow). (g) axial DWI demonstrates restricted diffusion (green arrow), DCE Initial rapid enhancement followed by a plateau. (Type 2 curve (h) (yellow arrow)). Management: (Surgical) Laparptomy was done with radical removal TAH & BSO, O-RADS MRI score: 4 Pathological diagnoses: Malignant mucinous cystadenocarcinoma.

Table 2 shows the distribution of ORADS MRI score among 50 participants revealed the most frequently assigned category with score 4 (38%), followed by score 5 (30%), score 3c (18%) and score 2 (14%).

Table (2): O- RADS MRI score among the studied participants (n=50)

O-RADS MRI score	No. of the studied participants=50	
	No.	%
2	7	14.0
3	9	18.0
4	19	38.0
5	15	30.0

In this prospective study, 90% of participants underwent histopathological analysis while 10% were managed by imaging follow up, of all cases 68% were confirmed malignant and 32% benign.

In this study a statistically sig. diff. was observed in adnexal lesion morphology between benign and malignant cases ($p<0.001$). Specifically large solid portion (no dark T2 dark in DWI areas) was predominantly seen in malignant lesions (55.9%), in contrast cystic lesions without solid component were more common in benign lesions.

Table 3 shows that there were no statistically significant differences in ORADS MRI scores between benign and malignant lesions ($p<0.001$). Score 4 and 5 were strongly associated with malignant pathology (94.1% of malignant cases), while score 2 and 3 were predominantly seen in benign lesions (87.6 %).

Table (3): Agreement between O- RADS MRI score classification and pathology among studied participants

ORADS MRI score	Pathology		Test of significance	P value	Kappa agreement
	Benign (n=16)	Malignant (n=34)			
	No. (%)	No. (%)			
Benign	14 (87.5)	2 (5.9)	33.31	**<0.001***	0.816
Malignant	2 (12.5)	32 (94.1)			

*: Statistically significant, $\chi 2$: Chi-squared test.

Interpretation: Perfect agreement

This study demonstrated that there was a false-negative case, one was scored as O-RADS MRI 3 (suggestive of benign lesion), as MRI revealed a multilocular cystic lesion with no solid components or suspicious enhancement. However, histopathological analysis revealed a juvenile granulosa cell tumor, a rare malignant sex- cord stromal tumor **(Figure 3)**.

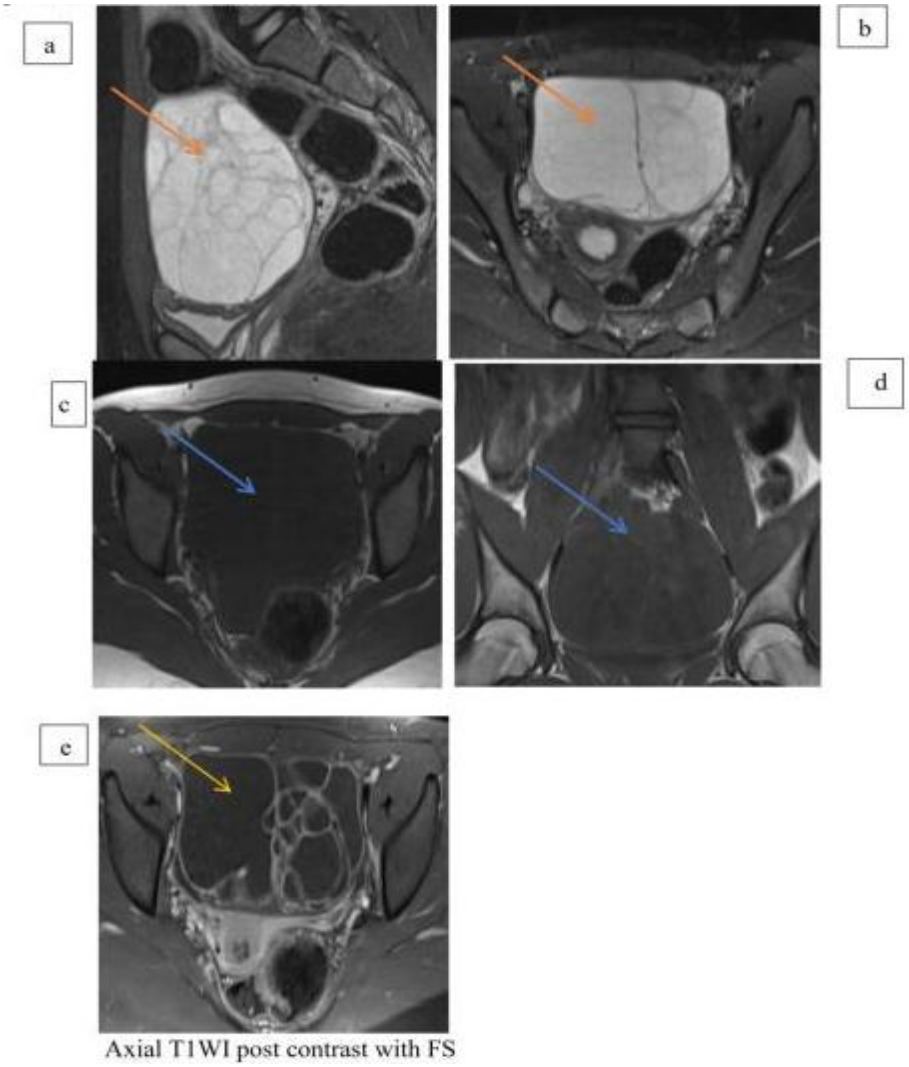

Figure (3): Female patient 12-year-old complain from pelvic pain, us showed multiloculated adnexal cystic lesion, MRI showed multiloculated cystic lesion with (a,b) sagittal and coronal T2WI hyper intense separated by thin septation(orange arrow), on (c,d) axial and coronal T1WI it appears hypointense with iso to hypointense septation(blue arrow),(e) post contrast axial T1 WI fat sat thin septal and wall enhancement(yellow arrow), ORADS MRI score 3, histopathology is jevunile granulosa cell tumor (JGCT).

Another case was pathologically diagnosed as a serous borderline ovarian tumor. MRI revealed a multiloculated cystic adnexal lesion with peripheral regular mural nodules. There was evidence of mild restricted diffusion on DWI, and the time-intensity curve (TIC) was of type I, indicating a benign enhancement pattern. According to the O- RADS MRI scoring system, the lesion was assigned score 3, as benign nature **(Figure 4).**

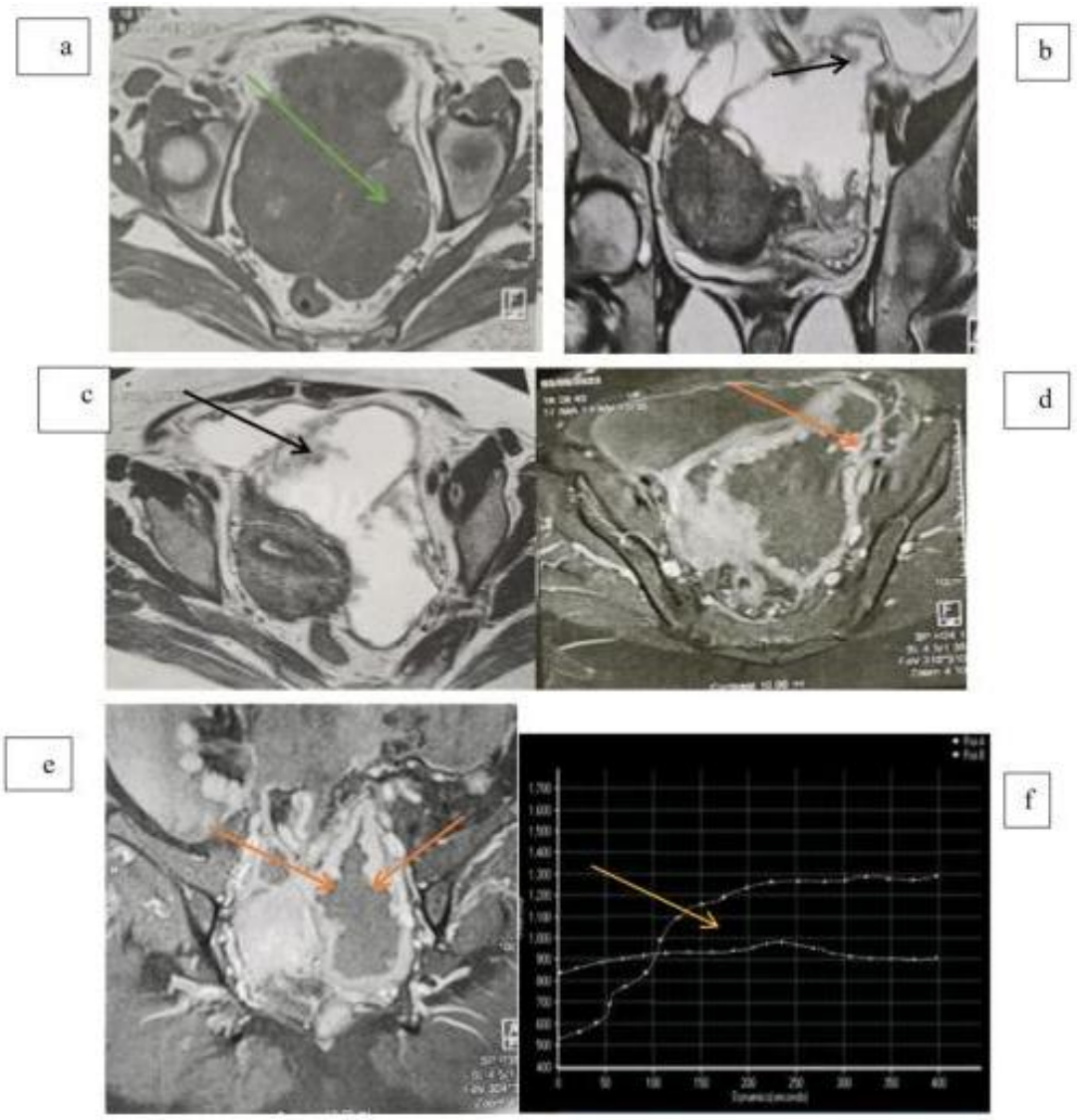

Figure (4): The 45-years-old female patient presented with abdominal pain, US showed bilateral adnexal complex lesions, MR Description: bilateral adnexal complex masses predominantly cystic, (a) axial T1WI low signal (green arrow), (b,c) coronal ,axial T2W1 high signal with peripheral regular mural nodules low T1 and low T2 (black arrow (b)), (d,e) axial and coronal T1WI fat sat post contrast enhancement of the peripheral regular mural nodules (orange arrow). DCE-MRI: Slow rising enhancement. Type 1 curve (f) (yellow arrow) ORADS MRI score: 3 Pathology: serous borderline tumor.

This study revealed statistically significant association between the type of management and the final pathological outcome (p=0.031) specifically 97.1% of malignant cases underwent surgical resection and pathological analysis compared to 75% of benign cases, while 25% of benign lesions were managed conservatively through follow up.

In this study we found that the PPV is 88%, and NPV of 94%. We found that the ROC curve analysis showed an area under the curve (AUC) of 0.949 with a 95% CI ranging from 0.885 to 1.000, which was statistically significant (p < 0.001) (**figure 5)**.

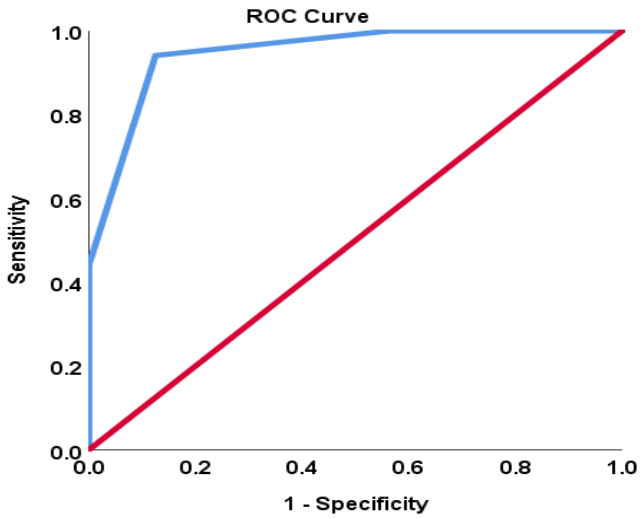

Figure (5): ROC curve analysis showed an area under the curve (AUC) of 0.949 with a 95% confidence interval (CI) ranging from 0.885 to 1.000, which was statistically significant (p < 0.001). Using a cut-off value of ≥ 4, the O-RADS MRI score achieved a sensitivity of 94%, specificity of 87% and accuracy of 92%.

Using a cut-off value of ≥ 4, the O- RADS MRI score achieved a sensitivity of 94%, specificity of 87%, accuracy of 92%, PPV of 88%, and NPV of 94%. **(Table 4)**

Table (4): Diagnostic accuracy of O- RADS MRI score in prediction of malignant lesion among studied participants

O- RADS MRI score	
AUC	**0.949**
95% CI	**0.885-1.000**
P value	**<0.001***
Cut off value	**≥ 4**
Sensitivity	**94%**
Specificity	**87%**
Accuracy	**92%**
PPV	**88%**
NPV	**94%**

**: Statistically significant, AUC: Area under curve, PPV: Positive predictive value, NPV: Negative predictive value, CI: Confidence interval.*

DISCUSSION

Ovarian lesions encompass a wide spectrum of conditions, ranging from benign cysts to malignant tumors originating from epithelial, germ cell, or stromal tissue. Accurate characterization is crucial to avoid unnecessary surgeries and ensure appropriate treatment [9]. MRI, with its superior soft tissue resolution and functional imaging sequences like DWI and DCE, plays a pivotal role in assessing adnexal masses, particularly when ultrasound findings are indeterminate [10].

The O-RADS MRI scoring system, developed by the ACR, integrates morphological and functional imaging features to stratify ovarian lesions from score 1 (normal ovary) to score 5 (high malignancy risk), thereby enhancing diagnostic consistency and guiding clinical decision-making [4].

This prospective study was conducted on 50 patients with ovarian lesions referred from gynecology to Menoufia University Hospitals. The mean age was 44.04 ± 17.51 years, similar to the EURAD cohort's 55.3±15.8 years in a study by **Wengert *et al.*** [11]. The most common presenting symptom was pelvic pain (70%), followed by abdominal swelling (32%) and urinary symptoms (16%), consistent with **Lamghare *et al.*** [12].

MRI findings showed most lesions were unilateral (68%), with a predominance of solid components lacking "dark–dark" features (40%), irregular septation or walls (28%), and peritoneal implants in 14%. These findings aligned with **Thomassin-Naggara *et al.*** [4], where 35% of lesions were solid or mixed and 12% had peritoneal implants. Type 2–3 time–intensity curves (TICs) were seen in most solid lesions, supporting intermediate-to-high malignancy suspicion.

O-RADS MRI scores were distributed as follows: score 4 (38%), score 5 (30%), score 3 (18%), and score 2 (14%). This mirrors distributions reported by **Thomassin-Naggara *et al.*** [4]**, Nougaret *et al.*** [13] **and Pereira *et al.*** [14] in tertiary care settings.

Of all cases, 90% underwent surgery with pathology confirmation, and malignancy was found in 68%, while 32% were benign, comparable to **Aslan *et al.*** [15]**,** who reported 63% malignancy in surgically selected cases.

Malignant lesions were significantly associated with older age (mean 49.3±18.3 vs. 32.9±8.7 years) and postmenopausal status (p= 0.001), echoing findings by **Sanaei *et al.*** [16] **and Sayasneh *et al.*** [17]. In contrast, symptoms such as pain or bleeding did not differ significantly between benign and malignant groups, consistent with **Mahaur *et al.*** [18] **and Thomassin-Naggara *et al.*** [4] who emphasized that clinical presentation alone is non-discriminatory.

Morphologically, "large solid portion without dark-dark areas" was more common in malignant lesions (55.9%) versus benign (6.3%), whereas purely

cystic patterns were more often benign. This reinforces findings by **Thomassin-Naggara *et al.* [4] and Spencer *et al.* [19]** on the malignant potential of solid lesions without dark signals on T2 or DWI.

O-RADS MRI scores were significantly predictive: scores 4–5 were seen in 94.1% of malignant lesions, while scores 2–3 were associated with 87.6% of benign lesions. These results confirm the system's diagnostic power, also reported in a meta-analysis by **Rizzo *et al.* [20].**

Surgical management correlated significantly with malignancy (p=0.031), reflecting clinical reliance on MRI findings. **Dabi *et al.* [21]** demonstrated that O-RADS MRI helped avoid unnecessary surgery in 88.2% of cases, endorsing surgical intervention for scores 4–5.

One borderline serous tumor was misclassified as O-RADS 3 due to imaging features suggestive of benignity (no solid enhancing components, type I TIC, mild diffusion restriction). This aligns with **Sahin *et al.* [22]** who noted borderline tumors can mimic benign cysts on MRI.

Similarly, a juvenile granulosa cell tumor (JGCT) appeared benign on MRI (O-RADS 3) but was confirmed as malignant by histopathology. **Boyraz *et al.* [23] and Afriliani & Wulanhandarini [24]** observed that JGCTs are often present as cystic lesions lacking solid features, complicating diagnosis. **Outwater & Siegelman[25]** also highlighted challenges with sex cord–stromal tumors mimicking benign lesions on MRI.

Our study demonstrated excellent diagnostic performance for O-RADS MRI, with an AUC of 0.949, sensitivity 94%, specificity 87%, and accuracy 92%. These values are in line with **Thomassin-Naggara *et al.* [4] and Basu *et al.* [26]. Aslan *et al.* [15]** also reported high diagnostic accuracy.

LIMITATIONS

Despite the promising results, this study has certain limitations. First, the sample size was relatively small (n=50), might restrict the generalizability of the results. Second, being a single-center study, the results may be influenced by institutional protocols or population characteristics. Additionally, follow-up data were limited for patients who did not undergo surgery, potentially affecting the final outcome classification. Future studies with larger, multicenter cohorts and standardized imaging protocols are warranted to validate and expand upon these findings.

CONCLUSION

It could be concluded that the O- RADS MRI scoring system is a reliable tool with high diagnostic performance in differentiating benign from malignant adnexal masses, with excellent sensitivity, specificity, and overall accuracy. Its structured approach and standardized lexicon facilitate uniform reporting and enhance communication between radiologists and clinicians, ultimately aiding in more informed and timely clinical decisions. Additionally, there is a strong concordance between our findings and those of multiple national and international studies.

RECOMMENDATION

We recommend that future studies be conducted as multicenter research with larger and more diverse patient populations to validate the diagnostic performance and generalizability of the O-RADS MRI system. We also advocate for the routine integration of O-RADS MRI into clinical practice to ensure standardized reporting, reduce inter-observer variability, and improve decision-making in patient management. Additionally, imaging findings should be correlated with histopathological outcomes or long-term clinical follow-up, particularly in indeterminate or high-risk cases. Structured training programs for radiologists and trainees are essential to enhance consistency and diagnostic accuracy in applying the O-RADS system. Furthermore, we recommend evaluating the role of advanced MRI techniques such as diffusion tensor imaging, perfusion imaging, and radiomics as potential tools to further improve the accuracy and specificity of adnexal mass characterization beyond current O-RADS criteria.

No funding.

No conflict of interest.

REFERENCES

1. **Foti P, Attinà G, Spadola S *et al.* (2016):** MR imaging of ovarian masses: classification and differential diagnosis. Insights Into Imaging, 7:21-41.
2. **Fischerova D, Burgetova A (2014):** Imaging techniques for the evaluation of ovarian cancer. Best Practice & Research Clinical Obstetrics & Gynaecology, 28(5):697-720.
3. **Forstner R, Thomassin-Naggara I, Cunha T *et al.* (2017):** ESUR guidelines: MR imaging of pelvic masses. European Radiology, 27(6): 2603–2627.
4. **Thomassin-Naggara I, Poncelet E, Jalaguier-Coudray A *et al.* (2020):** Ovarian-Adnexal Reporting Data System Magnetic Resonance Imaging (O-RADS MRI) score for risk stratification of sonographically indeterminate adnexal masses. JAMA Network Open, 3(1): e1919896. doi: 10.1001/jamanetworkopen.2019.19896.
5. **Shandley L, Spencer J, Kipling L *et al.* (2023):** The risk of infertility after surgery for benign ovarian cysts. Journal of Women's Health, 32: 574–582.
6. **Sisodia R, Del Carmen M (2022):** Lesions of the ovary and fallopian tube. New England Journal of Medicine, 387: 727–736.
7. **Sadowski E, Paroder V, Patel‐Lippmann K *et al.* (2018):** Indeterminate adnexal cysts at US: Prevalence and characteristics of ovarian cancer. Radiology, 287: 1041–1049.
8. **Alcázar J, Pascual M, Graupera B *et al.* (2016):** External validation of IOTA simple descriptors and

simple rules for classifying adnexal masses. Ultrasound in Obstetrics & Gynecology, 48(3): 397–402.

9. **Valentin L (2004):** Use of morphology to characterize and manage common adnexal masses. Best Pract Res Clin Obstet Gynaecol., 18(6):71–89.
10. **Thomassin-Naggara I, Daraï E, Nassar-Slaba J *et al.* (2011):** Value of dynamic contrast-enhanced MRI for distinguishing benign from malignant adnexal masses. Radiology, 258(3): 793–803.
11. **Wengert G, Dabi Y, Kermarrec E *et al.* (2022):** O-RADS MRI classification of indeterminate adnexal lesions: time-intensity curve analysis is better than visual assessment. Radiology, 303(3): 566-575.
12. **Lamghare P, Paidlewar S, Arkar R *et al.* (2024):** MRI Evaluation and Characterization of Ovarian Lesions Based on Ovarian-Adnexal Reporting and Data System MRI. Cureus, 16(8):e67904. doi: 10.7759/cureus.67904
13. **Nougaret S, Razakamanantsoa L, Sadowski E *et al.* (2024):** O-RADS MRI risk stratification system: pearls and pitfalls. Insights Into Imaging, 15(1): 45. doi: 10.1186/s13244-023-01577-5.
14. **Pereira P, Yoshida A, Sarian L *et al.* (2022):** Assessment of the performance of the O-RADS MRI score for the evaluation of adnexal masses, with technical notes. Radiologia Brasileira, 55: 137-144.
15. **Aslan S, Erol C, Inci E *et al.* (2023):** Diagnostic performance of O-RADS MRI score in the evaluation of adnexal masses: A single-center study. Acta Radiologica, 64(2): 229–236.
16. **Sanaei O, Hosseinpanah F, Rasti M (2020):** Age distribution and pathologic evaluation of women with adnexal masses: a prospective cohort study. Journal of Obstetrics and Gynaecology Research, 46(4): 567–574.
17. **Sayasneh A, Williamson K, Alkadhi H (2015):** Age and menopausal status as independent predictors in ovarian tumour triage: a prospective study. Ultrasound in Obstetrics & Gynecology, 45(4): 462–470.
18. **Mahaur A, Dutta P, Sirohi P (2024):** Clinical presentation of adnexal masses in reproductive-age women: a case–control study. Journal of Clinical Gynecology, 12(2): 123–130.
19. **Spencer J, Forstner R, Cunha T *et al.* (2010):** ESUR guidelines for MR imaging of the sonographically indeterminate adnexal mass: An algorithmic approach. European Radiology, 20(1): 25–35.
20. **Rizzo S, Cozzi A, Dolciami M *et al.* (2023):** O‐RADS MRI: A systematic review and meta‐analysis of diagnostic performance and category‐wise malignancy rates. Radiology, 307(1): e220795. doi: 10.1148/radiol.220795.
21. **Dabi Y, Rockall A, Razakamanantsoa L *et al.* (2024):** Management based on the O-RADS MRI scoring system could allow avoidance of non-essential surgery in 88.2% of cases. European Journal of Obstetrics & Gynecology and Reproductive Biology, 294: 135–142.
22. **Sahin H, Akdogan A, Smith J *et al.* (2021):** Serous borderline ovarian tumours: an extensive review on MR imaging features. British Institute of Radiology, 94(1125):20210116. doi: 10.1259/bjr.20210116.
23. **Boyraz B, Watkins J, Soubeyran I *et al.* (2022):** Cystic granulosa cell tumors of the ovary: An analysis of 80 cases of an often diagnostically challenging entity. Archives of Pathology & Laboratory Medicine, 146(12): 1450–1459.
24. **Afriliani N, Wulanhandarini T (2024):** Unusual radiologic imaging in juvenile granulosa cell tumor with precocious puberty: A unilocular cyst. Radiology Case Reports, 19(10): 4283–4288.
25. **Outwater E, Siegelman E (1997):** Ovarian fibromas and cystadenofibromas: MRI features of the fibrous component. Journal of Magnetic Resonance Imaging, 7(3): 465–471
26. **Basu A, Pame M, Bhuyan R *et al.* (2022):** Diagnostic performance of O-RADS MRI scoring system for the assessment of adnexal masses in routine clinical radiology practice: A single tertiary centre prospective cohort study. Journal of Clinical and Diagnostic Research, 16(4): 11–16.